Journal of Process Control 117 (2022) 169–180

Contents lists available at ScienceDirect

Journal of Process Control

journal homepage: www.elsevier.com/locate/jprocont

Robust state and input estimation with enhanced convergence rate for monitoring anaerobic digestion

Juan G. Rueda-Escobedo [a,*], Mihaela Sbarciog [b,c], Jaime A. Moreno [d,1], Jan Van Impe [b], Alain Vande Wouwer [e]

[a] Fachgebiet Regelungssysteme und Netzleitechnik, Brandenburgische Technische Universität Cottbus - Senftenberg, 03046 Cottbus, Germany
[b] Chemical & Biochemical Process Technology & Control (BioTeC+), Katholieke Universiteit Leuven, Gebroeders De Smetstraat 1, 9000 Gent, Belgium
[c] 3BIO-BioControl, Universite Libre de Bruxelles, CP 165/61, 50, Av. F.-D. Roosevelt, B-1050 Brussels, Belgium
[d] Coordinación de Eléctrica y Computación, Instituto de Ingeniería, 04510 Cd. Mx., Mexico
[e] Systems, Estimation, Control and Optimization (SECO), University of Mons, 7000 Mons, Belgium

ARTICLE INFO

Article history:
Received 13 December 2021
Received in revised form 28 June 2022
Accepted 27 July 2022
Available online xxxx

Keywords:
Super-twisting observer
Sliding mode observer
Asymptotic observer
State estimation
Unknown input observer
Waste treatment

ABSTRACT

In this study, an observer for estimating the state and unknown inputs is proposed for monitoring anaerobic digestion processes. This estimator is based on a dynamic model considering acidogenesis and methanogenesis, and consists of three sub-observers: (a) a gramian-based fixed-time convergent observer for the inlet chemical oxygen demand (COD) and the acidogenic bacteria population, (b) an asymptotic observer for the methanogenic bacteria population, and (c) a super-twisting observer for systems with time-varying parameters to estimate the inlet volatile fatty acid (VFA) concentration. These sub-observers can be designed independently, which greatly simplifies the tuning process. Proofs of convergence are developed and simulation tests show the performance of the estimation scheme as compared to classical extended Kalman filtering.

1. Introduction

Anaerobic digestion is nowadays a widespread technology for the treatment of organic waste or wastewater due to several advantages, including low energy requirement, reduced amount of biomass to be disposed and production of biogas, which can be used as a source of renewable energy. The complex biotransformations in anaerobic digestion are carried out by several groups of microorganisms, which convert the waste into biogas in several successive stages. A malfunction in any of these stages can lead to the failure of the entire process. Substantial efforts have been made to understand, model and control the process, which is sensitive to variations in the operating conditions. However, these efforts are hampered by the lack of on-line measurements of some key variables, which is a usual situation in waste treatment systems. Therefore, the missing information needs to be inferred by means of state/unknown input estimation techniques based on the available measurements and a dynamic model of the process.

For the anaerobic digestion process, two radically different levels of description are considered. On one hand, the detailed model ADM1 [1], with 26 state variables, is a gold standard for analyzing and simulating the process, but it is seldomly applied for developing state estimators due to its complexity and the amount of measurement required. For instance, [2] designs a robust interval observer to estimate 14 state variables using 10 measured variables, e.g., substrate concentrations and measurements related to biogas. On the other hand, low-order models, considering simple one-, two- or three-step reaction systems, such as the AMOCO (or AM2) [3], are often considered for the development of observers and controllers [4–8]. A major concern is the uncertainty on reaction kinetics, which can be alleviated by the use of asymptotic observers [9]. Various applications of this approach to anaerobic digestion systems have been reported [10]. Another concern is the absence of measurements of the influent composition, which led to the development of a great variety of unknown input observers. For instance, [4] presents an observer design based on a system transformation using a singular value decomposition, in order to estimate the unknown process inputs, e.g., concentrations of substrates and alkalinity in the influent, along with the unmeasured process states, e.g., acidogenic and methanogenic biomass concentrations and inorganic carbon, assuming that measurements of the chemical oxygen demand (COD), volatile fatty acids (VFA), alkalinity and

* Corresponding author.
E-mail addresses: ruedaesc@b-tu.de (J.G. Rueda-Escobedo), mihaela.iuliana.sbarciog@ulb.be (M. Sbarciog), jmorenop@iingen.unam.mx (J.A. Moreno), Jan.VanImpe@kuleuven.be (J. Van Impe), alain.vandewouwer@umons.ac.be (A.V. Wouwer).

[1] Jaime A. More wants to thanks the financial support from PAPIIT-UNAM, Mexico, Project IN102121.

https://doi.org/10.1016/j.jprocont.2022.07.014

outflow rates of methane and carbon dioxide are available. An interval observer for the unknown input of a one-step reaction anaerobic digestion model is derived in [11]. In [5], a virtually controlled observer is proposed to simultaneously estimate the influent substrate concentration and the unmeasured states of a two-step reaction anaerobic digestion model from measurements of the effluent COD, VFA and carbon concentrations. In [6], the authors designs an adaptive observer that exploits the cascade structure of the model to estimate the state vector and the maximum growth rate of the acidogenic and methanogenic biomass, using measurements of the COD and VFA concentrations. In [12], a continuous–discrete extended Kalman filter is proposed to estimate a slowly varying unknown input.

This brief (and by no means exhaustive) overview shows that measurements of the substrates within the reactor (chemical oxygen demand and volatile fatty acids) as well as measurements of the biogas (flow rate and composition) are often considered as information source. On the other hand, acidogenic and methanogenic biomass populations as well as influent concentrations are often out of reach and require some form of estimation.

The contribution of this work is to propose an integrated solution for the state and input estimation of a two-step anaerobic digestion model. The proposed solution relies on the use of sliding mode observers, which have been successfully applied to several biotechnological processes. For example, [13–15] employ second order sliding mode observers to estimate reaction rates, while [16] tackles the global estimation problem of a bioreactor with isotonic or non-isotonic growth.

For the two-step anaerobic digestion model AM2, [7] presents a generalized super-twisting algorithm based on [17] to estimate the acidogenic and methanogenic biomass concentrations as well as the concentrations of organic substrate and volatile fatty acids in the influent. The study [7] is a proof of concept through numerical simulations, and does not provide proofs of convergence and a complete design procedure. The objective of the present work is to provide these missing points and a rigorous analysis of the proposed observer, while innovating in the estimation of the inlet substrate and the bacteria population involved in the acidogenesis step. Our proposed observer consists of three parts:

1. A sub-observer for the inlet substrate (inlet COD) and bacteria population involved in the acidogenesis step. Contrary to the preliminary work [7], the internal stability of this sub-observer is guaranteed. Furthermore, by taking advantage of a constructibility Gramian, the sub-observer converges in fixed-time.
2. An asymptotic sub-observer for the methanogenic bacteria population. Different from [7], in this note we provide the sub-observer rate of convergence.
3. A super-twisting sub-observer for systems with time-varying parameters to estimate the inlet substrate (inlet VFA) in finite-time.

Since each sub-observer can be designed and tuned independently, the observation task is greatly simplified. For each sub-observer the convergence proof is presented and simulation results are included to illustrate the accuracy of the estimation.

This paper is organized as follows. Section 2 presents the anaerobic digestion system and the unknown input and state estimation problem. Section 3 develops the three-step observation scheme, while the several formal proofs are provided in Appendix A. The performance of the estimator is tested in simulation in Section 4 and compared to a classical extended Kalman–Bucy filter. Finally, the last section draws conclusions and perspectives.

1.1. Notation

$\mathbb{R}$ denotes the set of real numbers and $\mathbb{R}_{\geq 0}$ the set of non-negative real numbers, $\mathbb{R}^n$ the n-dimensional Euclidean space, and $\mathbb{R}^{n\times m}$ the set of $n \times m$ matrices. The symbol $\mathbf{I}_n \in \mathbb{R}^{n\times n}$ denotes the identity matrix. For symmetric matrices $A, B \in \mathbb{R}^{n\times n}$, $A > B$ ($A \geq B$) means that $A - B$ is positive (semi) definite. For $p \geq 1$, $\|v\|_p$ denotes the $p-$norm defined as $\left(\sum_{i=1}^{n} |v_i|^p\right)^{1/p}$. In the case of $B \in \mathbb{R}^{m\times n}$, $\|B\|_p$ denotes the induced norm of B, defined as $\sup_{\|v\|_p=1} \|Bv\|_p$. If the subscript is omitted, it denotes the Euclidean norm, i.e., $\|v\| = \|v\|_2$ and $\|B\| = \|B\|_2$. For a symmetric matrix A, $\lambda_{\min}(A)$ and $\lambda_{\max}(A)$ denote the smallest and largest eigenvalues of A, respectively. The elements below the diagonal of a symmetric matrix are denoted by $\star$. Finally, for $x \in \mathbb{R}$ and $p \geq 0$, $\lceil x \rfloor^p$ denotes the signed power of x, i.e., $|x|^p \mathrm{sign}(x)$. If $x \in \mathbb{R}^n$, then $\lceil x \rfloor^p$ is understood element-wise.

1.2. Definitions

Consider the time-varying system

$$\dot{x}(t) = f\big(x(t), t\big), \tag{1}$$

where $x(t) \in \mathbb{R}^n$. It is assumed that for every initial time $t_0 \geq 0$ and initial condition $x(t_0) \in \mathbb{R}^n$, the corresponding solution to (1) exists for all $t \geq t_0$ and it is unique. Suppose that $f(0, t) = 0$ for all $t \geq t_0 \geq 0$. We introduce the following concepts of Lyapunov stability.

Definition 1 (*Global Uniform Finite-Time Stability [18]*)**.** The solution $x(t) = 0$ of (1) is (Lyapunov) globally uniformly finite-time stable if, for each $\epsilon > 0$, there is $\delta(\epsilon) > 0$, independent of t_0, such that $\|x(t_0)\|_p < \delta$, with $p \geq 1$, implies that $\|x(t)\|_p < \epsilon$, and there is a function $T : \mathbb{R}_{\geq t_0} \times \mathbb{R}^n \to \mathbb{R}_{\geq 0}$, called *the settling time function*, such that, for every $t_0 \in \mathbb{R}_{\geq 0}$ and $x_0 \in \mathbb{R}^n$, $\lim_{t\to T(t_0,x_0)} x(t) = 0$ with $x(t_0) = x_0$.

Definition 2 (*Uniform Fixed-Time Stability [19]*)**.** The solution $x(t) = 0$ of (1) is (Lyapunov) uniformly fixed-time stable if it is (Lyapunov) globally uniformly finite-time stable and the settling time function is bounded, i.e., there exists $\bar{T} > 0$ such that $T(t_0, x_0) \leq \bar{T}$ for all $x_0 \in \mathbb{R}^n$ and $t_0 \geq 0$.

2. Anaerobic digestion model and problem statement

Consider an anaerobic digestion process taking place in a continuous flow stirred-tank bioreactor, characterized by two reactions [3]:

- Acidogenesis $as_1 \to x_1 + cs_2$,
- Methanogenesis $bs_2 \to x_2 + \mathrm{CH_4}$,

where $\mathrm{CH_4}$ denotes methane gas, s_1 is the organic substrate (COD) consumed by the acidogenic bacteria x_1, s_2 is the VFA converted by the methanogenic microorganisms x_2 into methane, and the positive constants a, b, and c are stoichiometric coefficients.

The mathematical model describing the process consists of the mass balance equations for the two species and the two substrates, together with the methane outflow rate. This results in the following five equations [3]:

$$\begin{aligned}
\dot{s}_1(t) &= u(t)\big(\sigma_1(t) - s_1(t)\big) - a\mu_1\left(s_1(t)\right)x_1(t),\\
\dot{x}_1(t) &= \big(\mu_1\left(s_1(t)\right) - u(t)\big)x_1(t),\\
\dot{s}_2(t) &= u(t)\big(\sigma_2(t) - s_2(t)\big) + c\mu_1\left(s_1(t)\right)x_1(t)\\
&\quad - b\mu_2\left(s_2(t)\right)x_2(t),\\
\dot{x}_2(t) &= \big(\mu_2\left(s_2(t)\right) - u(t)\big)x_2(t),\\
Q_M(t) &= q\,\mu_2\left(s_2(t)\right)x_2(t),
\end{aligned} \tag{2}$$

where $u(t) \in \mathbb{R}_{\geq 0}$ is the dilution rate (the ratio between the input flow and the reactor volume); $s_1(t) \in \mathbb{R}_{\geq 0}$, $s_2(t) \in \mathbb{R}_{\geq 0}$, $x_1(t) \in \mathbb{R}_{\geq 0}$ and $x_2(t) \in \mathbb{R}_{\geq 0}$ correspond to the system states; $Q_M(t)$ denotes the methane outflow rate with $q > 0$ the methane yield coefficient. Finally, the growth rates are denoted by $\mu_1 : \mathbb{R}_{\geq 0} \to \mathbb{R}_{\geq 0}$ and $\mu_2 : \mathbb{R}_{\geq 0} \to \mathbb{R}_{\geq 0}$ whereas the substrate concentrations in the influent are represented by $\sigma_1(t) \in \mathbb{R}_{\geq 0}$ (COD) and $\sigma_2(t) \in \mathbb{R}_{\geq 0}$ (VFA).

Based on available instrumentation (as described in [20]), it is assumed in the sequel that the substrates $s_1(t)$ and $s_2(t)$ are measured together with the methane outflow rate:

$$\begin{aligned} y_1(t) &= s_1(t), \\ y_2(t) &= s_2(t), \\ y_3(t) &= Q_M(t) = q\,\mu_2\left(s_2(t)\right) x_2(t). \end{aligned} \tag{3}$$

The main objective of this work is to design an observer for the system (2) with outputs (3) to reconstruct the species concentrations in the bioreactor $x_1(t)$ and $x_2(t)$, while considering the substrate concentrations at the inlet $\sigma_1(t)$ and $\sigma_2(t)$ as unknown inputs. An additional goal is to provide an estimate of $\sigma_1(t)$ and $\sigma_2(t)$. To this end, we assume that part of the bioreactor model (2) together with its parameters are known, according to:

Assumption 1.

1. The dilution rate $u(t)$, i.e., the system input, is known, and there exists $u_{\max} > 0$ such that $u_{\max} \geq u(t)$ for all $t \geq t_0$, i.e., $u(t)$ is uniformly bounded.
2. The stoichiometric coefficients of the model a, c and b are known together with the methane yield coefficient q.
3. The growth rate μ_1 is a known function of the substrate $s_1(t)$.
4. The growth rate μ_2 is an unknown function, continuous in its argument.

To account for the unknown substrate concentrations at the inlet, the following characterizations of $\sigma_1(t)$ and $\sigma_2(t)$ are introduced.

Assumption 2.

1. The substrate concentration at the influent $\sigma_1(t)$ is constant.
2. The substrate concentration at the influent $\sigma_2(t)$ is a smooth function of time such that its derivative is bounded by the dilution rate magnitude, i.e.,

   $$|\dot{\sigma}_2(t)| \leq L u(t) \quad \forall\, t \geq t_0,$$

   for some known constant $L > 0$.

Note that only an explicit model for μ_1 is required, whereas μ_2 is unknown. This is due to the availability of $y_3(t)$ which provides indirect information about μ_2, replacing the requirement of a model for it. Regarding Assumption 2, the first item assigns a model to σ_1 which allows to study its observability, whereas the second item means that the concentration at the influent $\sigma_2(t)$ can only change as long as there is media flowing into the bioreactor, and that its rate of change is not arbitrarily fast.

In the following, three sub-observers are designed to reconstruct the internal state of the bioreactor (2) together with the substrate concentrations at the influent σ_1 and $\sigma_2(t)$.

3. Observation scheme and main result

Before starting the observer design, we introduce the following auxiliary variables with the intention of simplifying the developments:

$$\begin{aligned} z(t) &:= \frac{c}{a} s_1(t) + s_2(t) = \frac{c}{a} y_1(t) + y_2(t), \\ \zeta(t) &:= \frac{c}{a} \sigma_1(t) + \sigma_2(t). \end{aligned} \tag{4}$$

Using the auxiliary variables $z(t)$ and $\zeta(t)$, the bioreactor dynamics (2) can be rewritten as

$$\begin{cases} \dot{s}_1(t) &= u(t)\big(\sigma_1(t) - s_1(t)\big) - a\mu_1\left(s_1(t)\right) x_1(t), \\ \dot{x}_1(t) &= \big(\mu_1\left(s_1(t)\right) - u(t)\big) x_1(t), \end{cases} \tag{5a}$$

$$\dot{x}_2(t) = \big(\mu_2\left(s_2(t)\right) - u(t)\big) x_2(t), \tag{5b}$$

$$\dot{z}(t) = u(t)\big(\zeta(t) - z(t)\big) - \tfrac{b}{q} y_3(t). \tag{5c}$$

Whereas (5a) and (5b) are taken directly from (2), (5c) is derived by taking the time derivative of $z(t)$ in (4), while considering the definitions of $y_3(t)$ in (3) and $\zeta(t)$ in (4). Note that by reconstructing $s_1(t)$, $\sigma_1(t)$, $z(t)$ and $\zeta(t)$, one can estimate $s_2(t)$ and $\sigma_2(t)$ using the inverse to (4), i.e.,

$$\begin{aligned} s_2(t) &= z(t) - \frac{c}{a} s_1(t), \\ \sigma_2(t) &= \zeta(t) - \frac{c}{a} \sigma_1(t). \end{aligned} \tag{6}$$

Therefore, the representations (2) and (5) are equivalent.

Based on the subsystems in (5), a three-step estimation scheme is developed in the sequel, that can be summarized as follows:

1. sub-observer 1, developed in Section 3.1, estimates in uniform fixed-time $s_1(t)$, $x_1(t)$ and $\sigma_1(t)$ in (5a) under the *uniform complete constructibility* of a linear time-varying system based on (5a).
2. sub-observer 2, exposed in Section 3.2, estimates $x_2(t)$ exponentially whenever the dilution rate $u(t)$ satisfies the classic *persistence of excitation* condition.
3. sub-observer 3, presented in Section 3.3, provides estimates in uniform finite-time of $z(t)$ and $\zeta(t)$. Together with the estimates provided by sub-observer 1, $\sigma_2(t)$ can be reconstructed using relationships (6).

3.1. Observer for the subsystem (5a)

Consider the (virtual) linear time-varying (LTV) system

$$\begin{aligned} \dot{\chi}(t) &= A(t)\chi(t), \\ \bar{y}_1(t) &= C\chi(t), \end{aligned} \tag{7}$$

with

$$\chi(t) = \begin{bmatrix} \chi_1(t) & \chi_2(t) & \chi_3(t) \end{bmatrix}^\top,$$

$$A(t) = \begin{bmatrix} -u(t) & -a\mu_1\big(y_1(t)\big) & u(t) \\ 0 & \mu_1\big(y_1(t)\big) - u(t) & 0 \\ 0 & 0 & 0 \end{bmatrix},$$

$$C = \begin{bmatrix} 1 & 0 & 0 \end{bmatrix}.$$

Note that the system (7) is driven by the input $u(t)$ and output $y_1(t)$ of (5a). Furthermore, iff (7) is initialized at the initial conditions of (5a), and under Assumption 2. 1, the trajectories and output of (7) reproduce the ones of (5a). This follows from the matching of the time derivative and the initial conditions. Thus, an observer for (7) also provides the estimates for $x_1(t)$ and σ_1 by recognizing that $\chi_1(t) = s_1(t)$, $\chi_2(t) = x_1(t)$ and $\chi_3(t) = \sigma_1$ for all $t \geq t_0$. By transitivity, this also implies that $\bar{y}_1(t) \equiv y_1(t)$. Moreover, this reveals conditions under which it is possible to reconstruct the state of (5a). These conditions are summarized in the following assumption.

Assumption 3. Consider systems (5a) and (7). We assume the existence of positive constants $\eta_1 \geq \eta_2$ and T_1, all independent of time, such that

$$\eta_1 \mathbf{I}_3 \geq \mathcal{C}(t, t-T_1) := \int_{t-T_1}^{t} \Phi^\top(s,t) C^\top C \Phi(s,t) \mathrm{d}s \geq \eta_2 \mathbf{I}_3, \tag{8}$$

where $\Phi(s,t)$ is the state transition matrix associated to $A(t)$, with $A(t)$ and C as in (7), and where $\mathcal{C}(t, t-T_1)$ is the constructibility Gramian of (7).

Assumption 3 is equivalent to the *uniform complete constructibility* of (7). Note also that uniform complete constructibility and uniform complete observability are equivalent for continuous time linear systems. Therefore, under Assumption 3, it is possible to estimate the internal state of (7), and thus the one of (5a).

To simplify the design and presentation of an observer for (5a), we introduce the invertible time-varying change of coordinates

$$\varsigma(t) = \begin{bmatrix} 1 & 0 & 0 \\ -1 & -a & \xi(t) \\ 0 & 0 & 1 \end{bmatrix} \chi(t), \tag{9}$$

where $\xi(t)$ is a known term generated by the auxiliary filter

$$\dot{\xi}(t) = -u(t)\xi(t) + u(t), \;\; \xi(t_0) \geq 0. \tag{10}$$

This results in the transformed system

$$\begin{aligned} \dot{\varsigma}(t) &= \bar{A}(t)\varsigma(t), \\ \bar{y}_1(t) &= C\varsigma(t), \end{aligned} \tag{11}$$

with

$$\bar{A}(t) = \begin{bmatrix} -u(t) + \mu_1(y_1(t)) & \mu_1(y_1(t)) & u(t) - \mu_1(y_1(t))\xi(t) \\ 0 & -u(t) & 0 \\ 0 & 0 & 0 \end{bmatrix}.$$

The transformation (9) not only preserves the upper triangular structure of (7), but now the elements in the main diagonal of $\bar{A}(t)$ are non-positive or can be rendered non-positive with an output injection. Furthermore, the structure of $\bar{A}(t)$ suggests that a linear output injection term can be used to introduce dissipation in the estimation error dynamics, thus stabilizing it. Using the system description (11), we propose the following observer:

$$\begin{aligned} \dot{\hat{\varsigma}}(t) = \bar{A}(t)\hat{\varsigma}(t) - K(t)\big[C\hat{\varsigma}(t) - y_1(t)\big] \\ - N(t)\sum_{i=1}^{2} r_i \big\lceil N(t)\hat{\varsigma}(t) - \psi(t)\big\rfloor^{p_i}, \end{aligned} \tag{12}$$

where $\hat{\varsigma}(t)$ is the estimate of $\varsigma(t)$, $r_1 > 0$ and $r_2 > 0$ are the observer gains, and the exponents $p_1 \in [0,1)$ and $p_2 > 1$ are design parameters. The linear output injection gain $K(t)$ is given by

$$K(t) = \big[\kappa_1 + \mu_1(y_1(t)) \;\; \mu_1(y_1(t)) \;\; u(t) - \mu_1(y_1(t))\xi(t)\big]^\top \tag{13}$$

with $\kappa_1 \geq 0$. Finally, the auxiliary variables $N(t) = N^\top(t)$ and $\psi(t)$ are generated by the filters

$$\begin{aligned} \dot{N}(t) &= -\bar{A}^\top(t)N(t) - N(t)\bar{A}(t) - N(t)QN(t) + C^\top C, \\ \dot{\psi}(t) &= -\big(\bar{A}(t) + QN(t)\big)^\top \psi(t) + C^\top y_1(t), \end{aligned} \tag{14}$$

with initial conditions $N(t_0) = 0$ and $\psi(t_0) = 0$, and where $Q = Q^\top > 0$ is a design parameter. Note that for any $Q > 0$, $N(t)$ is uniformly bounded since the pair $(-\bar{A}^\top(t), Q^{\frac{1}{2}})$ is always uniformly completely observable [21].

In (12), the linear output injection is used to stabilize the estimation error dynamics, and ensures the observer internal stability even when Assumption 3 is not satisfied. On the other hand, the nonlinear injection terms, depending on the exponents p_1 and p_2, are used to accelerate the convergence rate when Assumption 3 holds. The properties of the proposed observer are given in the following theorem.

Theorem 1. *Consider system (11) and observer (12). Let $u(t)$ be uniformly bounded. Define the estimation error as $\tilde{\varsigma}(t) = \hat{\varsigma}(t) - \varsigma(t)$. For any positive design parameters r_1, r_2, $p_1 \in [0,1)$, $p_2 > 1$, $\kappa_1 \geq 0$, and positive definite symmetric matrix Q, the solution $\tilde{\varsigma}(t) = 0$ of the estimation error dynamics is globally uniformly stable. Furthermore, if Assumption 3 is satisfied, the solution $\tilde{\varsigma}(t) = 0$ is uniformly fixed-time stable (see Definition 2), meaning that $\hat{\varsigma}(t)$ converges to $\varsigma(t)$ in fixed-time, uniformly in t_0.*

Finally, the estimate of the original states is given by

$$\begin{bmatrix} \hat{s}_1(t) \\ \hat{x}_1(t) \\ \hat{\sigma}_1(t) \end{bmatrix} = \begin{bmatrix} 1 & 0 & 0 \\ -1/a & -1/a & \xi(t)/a \\ 0 & 0 & 1 \end{bmatrix} \hat{\varsigma}(t),$$

with $\xi(t)$ as in (10), and for any $\xi(t_0) \geq 0$.

Remark 1. The convergence time of the proposed observer (12) depends on the chosen observer parameters, the excitation level η_2 in (8), and it cannot be less than the constructibility window length, i.e., $T_1 > 0$ in (8).

Assumption 3 provides sufficient conditions for estimating the state of (7) together with σ_1. However, it does not give direct conditions over $u(t)$ and $y_1(t)$ to verify whenever Assumption 3 holds. We investigate this in the following proposition.

Proposition 1. *Let $u(t)$ and $\mu_1(y_1(t))$ be uniformly bounded. The system (7) is uniformly completely observable iff there exist positive constants γ_1, γ_2 and T_1, all independent of time, such that*

$$\gamma_1 \mathbf{I}_2 \geq \int_{t}^{t+T_1} \mathcal{K}^\top(s,t)\mathcal{K}(s,t)\mathrm{d}s \geq \gamma_2 \mathbf{I}_2, \tag{15}$$

with

$$\begin{aligned} \mathcal{K}(s,t) &= \int_t^s B(\sigma, t)\mathrm{d}\sigma, \\ B^\top(t, t_0) &= \begin{bmatrix} -\mu_1(y_1(t)) \exp\Big(-\int_{t_0}^{t} u(\sigma)\mathrm{d}\sigma\Big) \\ u(t) - \mu_1(y_1(t)) \end{bmatrix}. \end{aligned} \tag{16}$$

The observer (12) together with Theorem 1 provide the machinery required for estimating a constant unknown input σ_1. Furthermore, under Assumption 3, and due to the robustness of the fixed-time convergence, disturbances such as noise or variations in σ_1 will result in bounded estimation errors. This point is illustrated in Section 4 via numerical simulation.

3.2. Observer for the subsystem (5b)

With the purpose of designing an observer for the subsystem (5b), we use the output $y_3(t)$ in (3) to rewrite (5b) as

$$\dot{x}_2(t) = -u(t)x_2(t) + \frac{1}{q}y_3(t). \tag{17}$$

Once the system is in the form (17), it is possible to use a copy of the system dynamics as an observer since all the terms involved are known. Hence, the observer takes the form [7,9]

$$\dot{\hat{x}}_2(t) = -u(t)\hat{x}_2(t) + \frac{1}{q}y_3(t), \tag{18}$$

where $\hat{x}_2(t)$ is the estimate of $x_2(t)$. Thanks to the availability of $y_3(t)$, the observer (18) is independent of μ_2.

The observer (18) has the following properties.

Theorem 2. *Consider the system (17) and the observer (18). Let $u(t)$ be uniformly bounded, and define the estimation error as $\tilde{x}_2(t) = \hat{x}_2(t) - x_2(t)$. Then the solution $\tilde{x}_2(t) = 0$ of the estimation error dynamics is globally uniformly stable. Furthermore, if there exist positive constants γ_3, γ_4 and T_2, all independent of time, such that*

$$\gamma_3 \geq \int_{t-T_2}^{t} u^2(\tau)\mathrm{d}\tau \geq \gamma_4, \tag{19}$$

the solution $\tilde{x}_2(t) = 0$ is globally uniformly asymptotically stable, i.e., the estimate $\hat{x}_2(t)$ converges to $x_2(t)$ asymptotically, uniformly in t_0. In such case, the estimation error satisfies the bound

$$\left|\tilde{x}_2(t)\right| \leq \sqrt{\frac{\beta_1}{\beta_2}}\left|\tilde{x}_2(t_0)\right| \exp\left(-\frac{\gamma_4}{4\beta_2}\left(t-t_0\right)\right), \tag{20}$$

with

$$\beta_1 = \frac{2T_2^2 u_{\max}^2 \gamma_3^2}{\gamma_4} + T_2 + T_2\gamma_3, \qquad \beta_2 = \frac{2T_2^2 u_{\max}^2 \gamma_3^2}{\gamma_4} + T_2, \tag{21}$$

and where $u_{\max}$ is given in Assumption 1.

Note that (19) is required for the observer to converge. This condition means that the dilution rate $u(t)$ has to be *persistently exciting*. This happens, for example, when $u(t)$ does not approach asymptotically $u(t) = 0$. Also, note that the convergence rate (20) depends on the excitation level of $u(t)$, and that it cannot be improved by means of the observer parameters. This makes the proposed observer an *asymptotic observer* [9].

3.3. Observer for the subsystem (5c)

The subsystem (5c) can be understood as a system subject to the external disturbance $\zeta(t)$. Under Assumption 2. 2, it is possible to compensate the disturbance using a *super-twisting-like* algorithm, allowing to estimate both, the state $z(t)$ and the disturbance $\zeta(t)$, in finite time.

An important difference with respect to the standard application of the super-twisting algorithm is that the disturbance is multiplied by a time-dependent variable, in this case the dilution rate $u(t)$. Hence, we propose to use the super-twisting observer for systems with time-varying parameters presented in [22]. For the system (5c), the observer takes the form

$$\begin{aligned}
\dot{\hat{z}}(t) &= -k_1 u(t)\phi_1\left(\tilde{z}(t)\right) - \frac{b}{q}y_3(t) + u(t)\left(\hat{\zeta}(t) - z(t)\right), \\
\dot{\hat{\zeta}}(t) &= -k_2 u(t)\phi_2\left(\tilde{z}(t)\right),
\end{aligned} \tag{22}$$

with $\tilde{z}(t) = \hat{z}(t) - z(t)$ and

$$\begin{aligned}
\phi_1\left(\tilde{z}(t)\right) &= m_1\lceil\tilde{z}(t)\rfloor^{\frac{1}{2}} + m_2\lceil\tilde{z}(t)\rfloor^{p_3}, \\
\phi_2\left(\tilde{z}(t)\right) &= \frac{m_1^2}{2}\lceil\tilde{z}(t)\rfloor^{0} + m_1 m_2\left(p_3 + \frac{1}{2}\right)\lceil\tilde{z}(t)\rfloor^{p_3-\frac{1}{2}} \\
&\quad + m_2^2\lceil\tilde{z}(t)\rfloor^{2p_3-1}.
\end{aligned}$$

The algorithm parameters are the positive constants k_1, k_2, $p_3 \geq \frac{1}{2}$, m_1 and m_2. It holds that $\phi_2(\tilde{z}) = \phi_1'(\tilde{z})\phi_1(\tilde{z})$ [22]. Note also that ϕ_1 is continuous, whereas ϕ_2 is discontinuous at $\tilde{z} = 0$. Hence, the solutions of (22) have to be understood in the sense of Filippov [23].

For this observer, we have the following result.

Theorem 3. *Consider the system (5c) and the observer (22). Let $u(t)$ be uniformly bounded. Define the estimation errors as $\tilde{z}(t) = \hat{z}(t) - z(t)$ and $\tilde{\zeta}(t) = \hat{\zeta}(t) - \zeta(t)$. Fix the observer parameters $m_1 > 0$, $m_2 > 0$ and $p_3 \in [\frac{1}{2}, 1]$. Design the observer gains as*

$$k_1 = \frac{\rho_2 l_1 + l_2}{\rho_1\rho_2 - 1}, \qquad k_2 = \frac{l_1 + \rho_1 l_2}{\rho_1\rho_2 - 1}, \tag{23}$$

where $\rho_1 > 0$, $\rho_2 > 0$, $l_1 > 0$ and $l_2 \in \mathbb{R}$ are such that

$$\rho_1\rho_2 > 1, \; l_1 > \frac{2L}{m_1^2} + \frac{1}{4}\left(l_2 - \rho_1 \pm \rho_2\frac{2L}{m_1^2}\right)^2, \tag{24}$$

and with $L > 0$ as in Assumption 2. 2. Then the solution $\{\tilde{z}(t) = 0, \; \tilde{\zeta}(t) = 0\}$ of the estimation error dynamics is globally uniformly stable. Furthermore, if $u(t)$ satisfies (19) for some positive constants γ_3, γ_4, and T_2, all independent of time, the solution $\{\tilde{z}(t) = 0, \; \tilde{\zeta}(t) = 0\}$ is globally uniformly finite-time stable (see Definition 1). That is, the estimates $\hat{z}(t)$ and $\hat{\zeta}(t)$ converge to $z(t)$ and $\zeta(t)$, respectively, in finite time, uniformly in t_0.

The estimate of the original variables is given by

$$\begin{aligned}
\hat{s}_2(t) &= \hat{z}(t) - \frac{c}{a}y_1(t), \\
\hat{\sigma}_2(t) &= \hat{\zeta}(t) - \frac{c}{a}\hat{\sigma}_1(t),
\end{aligned}$$

where $\hat{\sigma}_1(t)$ is obtained from the observer (12).

3.4. Discussion

Splitting the bioreactor dynamics (2) for the observer design purpose results in several benefits. On one hand, it was possible to minimize the hypotheses over σ_2 and the knowledge of μ_2. In the case of σ_1, its estimation in combination with x_1 was investigated, and precise observability conditions were derived. Analogue results were also possible in the case of x_2. Second, specialized observers were developed for each subsystem, which in the case of $x_1(t)$, $\sigma_1(t)$ and $\sigma_2(t)$, provide enhanced convergence properties such as finite and fixed-time convergence. Third, the observers (12) and (22) can be tuned independently of (18), which allows decoupling the convergence of $\hat{x}_1(t)$, $\hat{\sigma}_1(t)$ and $\hat{\sigma}_2(t)$ from $\hat{x}_2(t)$. This contrasts with the standard application of the extended Kalman–Bucy filter, where it is difficult to independently tune the converge rate for each state. Finally, the uniform convergence properties obtained under the persistence of excitation conditions (15) and (19) guarantee robustness of the estimation process under additive disturbances such as noise or additional bounded unknown inputs [24, Sec. 4.9], [25].

In the next section, we illustrate the application of the proposed observation scheme, and show its enhanced convergence speed with respect to a Kalman–Bucy filter.

4. Simulation tests

The bioreactor model (2) is simulated using the stoichiometric coefficients, the growth functions μ_1 and μ_2, and the initial conditions from [8]. The growth rate functions μ_1 and μ_2 are of the Monod and Haldane type, respectively, and are described by

$$\mu_1(s_1) = \frac{\mu_1^{\max} s_1}{s_1 + K_{s_1}}, \quad \mu_2(s_2) = \frac{\mu_2^{\max} s_2}{\frac{1}{K_{I_2}}s_2^2 + s_2 + K_{s_2}}.$$

The stoichiometric coefficients together with the growth functions parameters are given in Table 1.

The influent substrate concentrations $\sigma_1(t)$ and $\sigma_2(t)$ are given by

$$\begin{aligned}
\sigma_1(t) &= 50, \\
\sigma_2(t) &= 82.5 + 10\sin(t) + 2\sin(5t) + \sin(10t).
\end{aligned} \tag{25}$$

Finally, to ensure enough excitation and satisfy the conditions of Assumption 3 and (19), the dilution rate is chosen as a squared

Table 1
Parameters of the simulated anaerobic digestor (2), following [8, Tab. 3].

Stoichiometric coefficients		Growth rate parameters	
a	100	$\mu_1^{\max}$	1 [d^{-1}]
b	300 [mmol/g]	K_{s_1}	5 [g/L]
c	280 [mmol/g]	$\mu_2^{\max}$	0.8 [d^{-1}]
q	500 [mmol/g]	K_{s_2}	60 [mmol/L]
		K_{I_2}	350 [mmol/L]

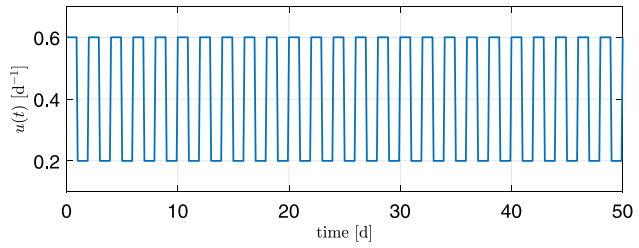

Fig. 1. Dilution rate used during the simulation.

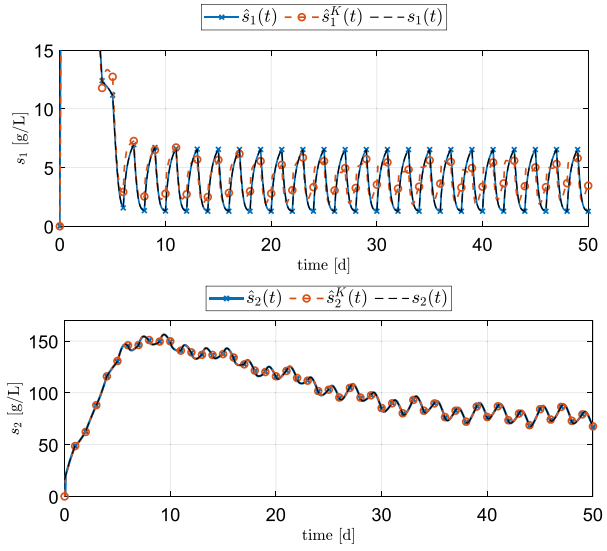

Fig. 2. Estimation of the organic substrate (COD) $s_1(t)$ and the VFA $s_2(t)$ by the proposed observation scheme, denoted by $\hat{s}_1(t)$ and $\hat{s}_2(t)$, and the extended Kalman–Bucy observer, denoted by $\hat{s}_1^K(t)$ and $\hat{s}_2^K(t)$.

wave with period 2 [d], amplitude 0.4 [d^{-1}], and with a bias term of 0.2 [d^{-1}]. A plot of the dilution rate is provided in Fig. 1.

The parameters of the observer (12) are chosen as

$$r_1 = r_2 = 5000,\ p_1 = 0,\ p_2 = 4,\ \kappa_1 = 1500,\ Q = 100\,\mathbf{I}_3.$$

For this observer, the convergence rate depends on the gains r_1 and r_2, and the exponents p_1 and p_2. To speed up the convergence, one can increase r_1, r_2, and p_2, or decrease p_1. For this example, we took the minimum for p_1, i.e., $p_1 = 0$, and a high but numerically stable value for p_2, i.e., $p_2 = 4$. The initial conditions for the observer, including the filter $\xi(t)$ in (10), are taken as zero. In the case of the second observer (18), there are no parameters to be set. Finally, for the third observer (22), we fix

$$m_1 = m_2 = 15, \quad \rho_1 = \rho_2 = l_2 = 2, \quad p_3 = 1.$$

Based on the description provided for $\sigma_2(t)$ in (25) and the minimum of $u(t)$, we estimate L as

$$L = 500 \geq \frac{\sup_{t\geq t_0} |\dot{\sigma}_2(t)|}{\min_{t\geq t_0} u(t)}.$$

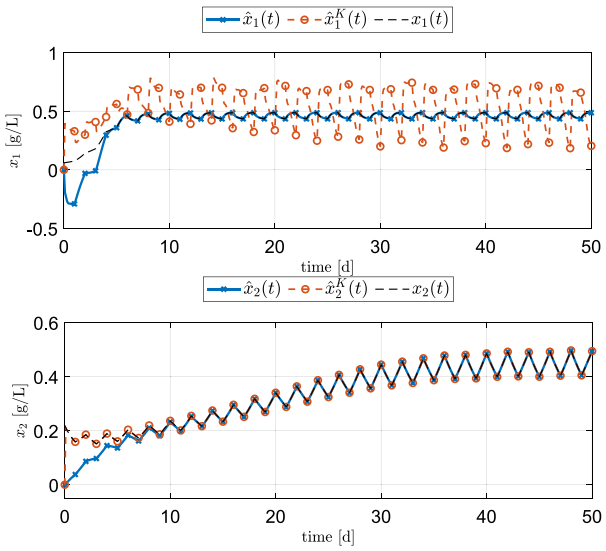

Fig. 3. Estimation of the acidogenic bacteria biomass $x_1(t)$ and the methanogenic microorganism biomass $x_2(t)$ by the proposed observation scheme, denoted by $\hat{x}_1(t)$ and $\hat{x}_2(t)$, and the extended Kalman–Bucy observer, denoted by $\hat{x}_1^K(t)$ and $\hat{x}_2^K(t)$.

In order to satisfy (24), and given $L = 500$, we choose $l_1 = 26.62$. This yields the observer gains $k_1 = 18.41$ and $k_2 = 10.21$.

To contrast the proposed observer scheme, an extended Kalman–Bucy filter is implemented taking as system matrices $\mathcal{A}(t)$ and $\mathcal{C}(t)$ in (27) (Eq. 27 is given in Box I). In such case, the observer is described by

$$\dot{\hat{X}}(t) = \mathcal{A}(t)\hat{X}(t) - H(t)\mathcal{C}^\top(t)R^{-1}\left(\mathcal{C}(t)\hat{X}(t) - \begin{bmatrix} y_1(t) \\ y_2(t) \\ y_3(t) \end{bmatrix}\right), \tag{26}$$

$$\hat{X}(t) = \begin{bmatrix} \hat{s}_1(t) & \hat{x}_1(t) & \hat{\sigma}_1(t) & \hat{s}_2(t) & \hat{x}_2(t) & \hat{\sigma}_2(t) \end{bmatrix}^\top,$$

with $H(t)$ the solution of the differential Riccati equation

$$\dot{H}(t) = \mathcal{A}(t)H(t) + H(t)\mathcal{A}^\top(t) - H(t)\mathcal{C}^\top(t)R^{-1}\mathcal{C}(t)H(t) + P,$$

with $R^{-1} = 10\,\mathbf{I}_3$, $P = \mathbf{I}_6$, and $H(t_0) = 100\,\mathbf{I}_6$. Note that, in contrast with the proposed observer scheme, for implementing the observer (26), the expression for μ_2 is required and the unknown input σ_2 has to be considered as a constant function.

The system of differential equations is solved using `Matlab©` `Simulink©` in combination with the solver `ode45` with a step size bounded in the interval $[10^{-7}, 10^{-5}]$ [d] ($[8.64\times10^{-3}, 0.864]$ [s]). The estimation results are shown in Fig. 2 for $s_1(t)$ and $s_2(t)$, in Fig. 3 for $x_1(t)$ and $x_2(t)$, and in Fig. 4 for $\sigma_1(t)$ and $\sigma_2(t)$. As can be seen in Fig. 2, the proposed observer correctly estimate $s_1(t)$ and $s_2(t)$, whereas the Kalman–Bucy filter presents an error in $s_1(t)$. Nevertheless, both observers provide an adequate estimation, which is not surprising since these variables are measured. The first important difference appears in the estimation of $x_1(t)$ in Fig. 3. Whereas the proposed observer correctly estimates $x_1(t)$, the estimate provided by the extended Kalman–Bucy filter oscillates around the correct value. By looking at Fig. 6, we can see that the relative error is as high as 65% at some points. In the case of the proposed observer, the relative error in x_1 vanishes after 5 days, as is shown in Fig. 5. In the case of $x_2(t)$, both observers provide an accurate estimation. However, we remark once more that the extended Kalman–Bucy filter requires the model of μ_2,

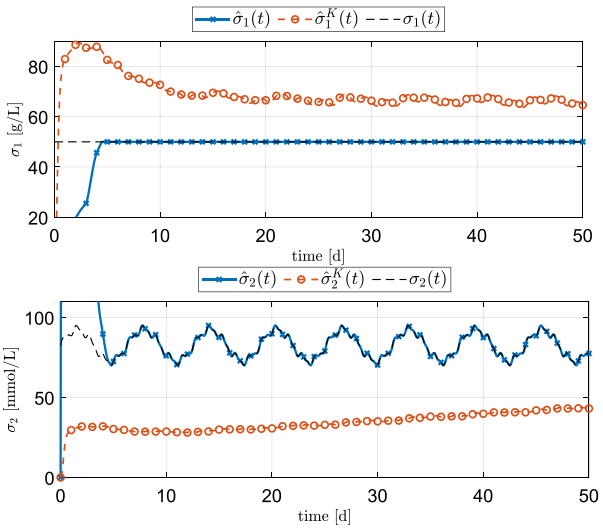

Fig. 4. Estimation of the substrate concentrations in the influent $\sigma_1(t)$ and $\sigma_2(t)$ by the proposed observation scheme, denoted by $\hat{\sigma}_1(t)$ and $\hat{\sigma}_2(t)$, and the extended Kalman–Bucy observer, denoted by $\hat{\sigma}_1^K(t)$ and $\hat{\sigma}_2^K(t)$.

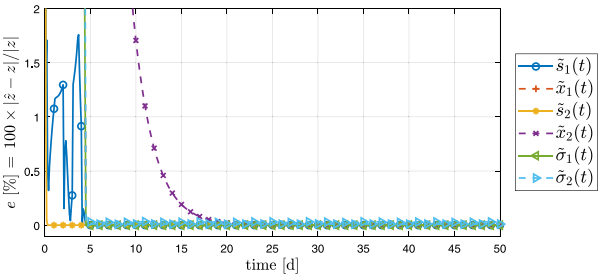

Fig. 5. Relative error in percentage per estimated variable with the proposed observation scheme.

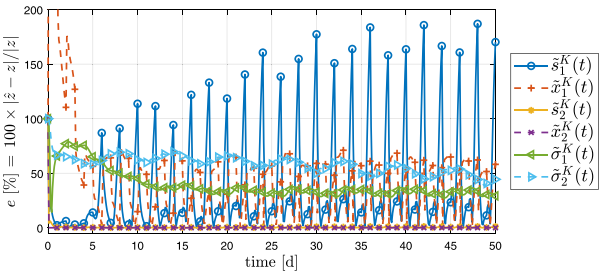

Fig. 6. Relative error in percentage per estimated variable with the extended Kalman–Bucy observer.

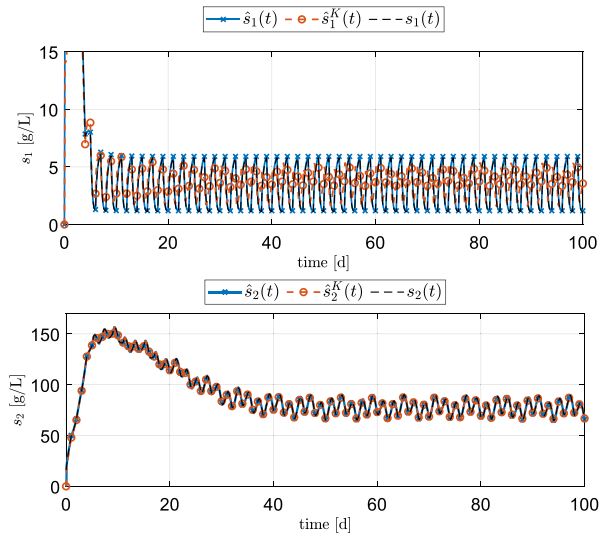

Fig. 7. Estimation of the organic substrate (COD) $s_1(t)$ and the VFA $s_2(t)$ by the proposed observation scheme, denoted by $\hat{s}_1(t)$ and $\hat{s}_2(t)$, and the extended Kalman–Bucy observer, denoted by $\hat{s}_1^K(t)$ and $\hat{s}_2^K(t)$, under disturbed conditions.

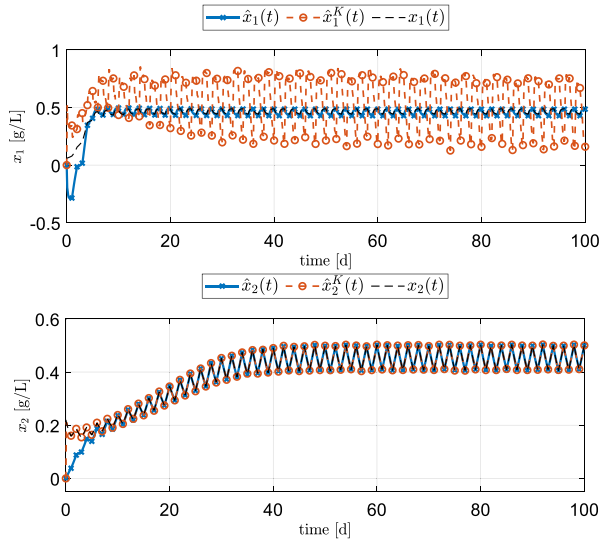

Fig. 8. Estimation of the acidogenic bacteria biomass $x_1(t)$ and the methanogenic microorganism biomass $x_2(t)$ by the proposed observation scheme, denoted by $\hat{x}_1(t)$ and $\hat{x}_2(t)$, and the extended Kalman–Bucy observer, denoted by $\hat{x}_1^K(t)$ and $\hat{x}_2^K(t)$, under disturbed conditions.

whereas the observer (18) is independent of it. Finally, for $\sigma_1(t)$ and $\sigma_2(t)$, only the proposed observation scheme is capable of providing an accurate estimation, as is shown in Fig. 4. In the case of the extended Kalman–Bucy filter, the relative error in $\sigma_1(t)$ stabilizes around 40%, while for $\sigma_2(t)$, the relative error oscillates around 50%. This is shown in Fig. 6. In the case of the proposed observation scheme, the relative error in both variables, $\sigma_1(t)$ and $\sigma_2(t)$, vanishes after 5 days, which can be seen in Fig. 5.

To show the robustness of the proposed approach, we repeated the simulation while adding uniform noise to the measurements. The noises added to the measurements $y_1(t)$, $y_2(t)$, and $y_3(t)$ in (3) are bounded in the intervals $[-0.05, 0.05]$, $[-4, 4]$, and $[-3, 3]$, respectively. The noise level introduced corresponds to 4∼5% of the signals magnitude on average. Furthermore, based on [26], we introduced a zero-order-hold in the measurements with a sampling time of 1.3×10^{-4} [d] (11.23 [s]) to emulate the sampling time of the sensors. Finally, we perturbed the model of μ_1 used in the bioreactor by taking $1.05\mu_1^{\max}$ and $0.95K_{s_1}$ instead of the original parameters. Note also that the value of μ_1 is computed using the noisy measurement $y_1(t)$. The results of the simulation with disturbances are shown in Figs. 7, 8, and 9. Overall, the proposed observer keeps a correct estimation of the bioreactor states and inputs under these circumstances, as shown by the relative errors in Fig. 10. In the case of the Kalman–Bucy filter, the previous errors in the estimates of $s_1(t)$, $x_1(t)$, $\sigma_1(t)$, and $\sigma_2(t)$ persist, as revealed by the relative errors in Fig. 11. Finally, to aid in the interpretation of the simulation results, we provide in Table 2 the RMS value of the relative errors shown in Figs. 10 and 11.

$$\mathcal{A}(t)=\begin{bmatrix} -u(t) & -a\,\mu_1(y_1(t)) & u(t) & 0 & 0 & 0\\ 0 & \mu_1(y_1(t))-u(t) & 0 & 0 & 0 & 0\\ 0 & 0 & 0 & 0 & 0 & 0\\ 0 & c\,\mu_1(y_1(t)) & 0 & -u(t) & -b\,\mu_2(y_2(t)) & u(t)\\ 0 & 0 & 0 & 0 & \mu_2(y_2(t))-u(t) & 0\\ 0 & 0 & 0 & 0 & 0 & 0 \end{bmatrix},\quad \mathcal{C}^{\top}(t)=\begin{bmatrix} 1 & 0 & 0\\ 0 & 0 & 0\\ 0 & 0 & 0\\ 0 & 1 & 0\\ 0 & 0 & q\,\mu_2(y_2(t))\\ 0 & 0 & 0 \end{bmatrix}. \tag{27}$$

Box I.

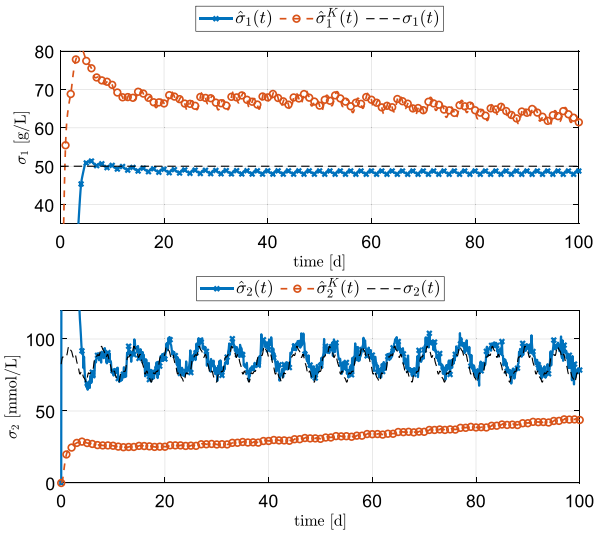

Fig. 9. Estimation of the substrate concentrations in the influent $\sigma_1(t)$ and $\sigma_2(t)$ by the proposed observation scheme, denoted by $\hat{\sigma}_1(t)$ and $\hat{\sigma}_2(t)$, and the extended Kalman–Bucy observer, denoted by $\hat{\sigma}_1^K(t)$ and $\hat{\sigma}_2^K(t)$, under disturbed conditions.

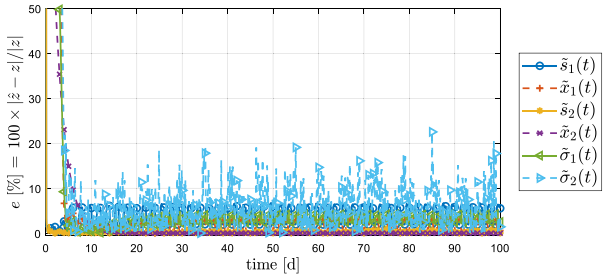

Fig. 10. Relative error in percentage per estimated variable with the proposed observation scheme under disturbed conditions.

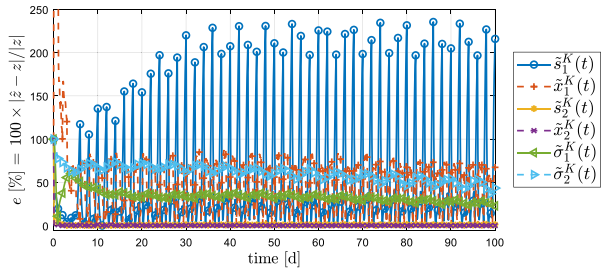

Fig. 11. Relative error in percentage per estimated variable with the extended Kalman–Bucy observer under disturbed conditions.

Table 2
RMS value of the relative errors shown in Figs. 10 and 11 after a transient of 10 [d].

Variable	$\tilde{s}_1$	$\tilde{x}_1$	$\tilde{s}_2$
Proposed observer	4.28%	1.66%	0.22%
Extended KBO	85.5%	53.8%	0.60%
Variable	$\tilde{x}_2$	$\tilde{\sigma}_1$	$\tilde{\sigma}_2$
Proposed observer	0.20%	3.0%	6.87%
Extended KBO	0.21%	32.3%	59.9%

5. Conclusions

In this work, a three-step observation scheme, consisting of a Gramian-based observer, an asymptotic observer, and a super-twisting observer, is developed to monitor an anaerobic digestion process based on the AM2 model. The sub-observers can be designed independently, and the overall scheme provides enhanced convergence and robustness with respect to an extended Kalman–Bucy filter. It is important to note that the step-by-step observer design presented in this study is not restricted to the anaerobic digestion system, but could also be extended to other systems with sequential reactions such as for instance nitrification–denitrification systems. Furthermore, the finite and fixed-time convergence provided by the proposed scheme is well suited for the monitoring of bioreactors operating in batch, where early estimates are crucial.

CRediT authorship contribution statement

Juan G. Rueda-Escobedo: Methodology, Software, Formal analysis, Writing – original draft. **Mihaela Sbarciog:** Conceptualization, Software, Investigation, Writing – original draft. **Jaime A. Moreno:** Conceptualization, Methodology, Formal analysis, Writing – review & editing. **Jan Van Impe:** Conceptualization, Funding acquisition. **Alain Vande Wouwer:** Conceptualization, Methodology, Resources, Investigation, Writing – review & editing.

Declaration of competing interest

The authors declare that they have no known competing financial interests or personal relationships that could have appeared to influence the work reported in this paper.

Appendix A. Proof of claims

A.1. Proof of Theorem 1

Before proving the central result, we need to show that the following two properties hold:

$$N(t)\varsigma(t)\equiv\psi(t)\qquad\forall\, t\geq t_0, \tag{A.1}$$

$$N(t)\geq\bar{\eta}\mathbf{I}_3>0\quad\forall\, t\geq t_0+T_1. \tag{A.2}$$

The first relation will be used to show that the nonlinear output injection in (12) carries information about the estimation error, whereas the second one means that $N(t)$ is positive definite with eigenvalues larger than $\bar{\eta} > 0$.

To prove (A.1), we consider the time derivative of $N(t)\varsigma(t)$, which taking into account (11) and (14), and by noticing that $\bar{y}_1(t) \equiv y_1(t)$ results in

$$\begin{aligned}\frac{\mathrm{d}}{\mathrm{d}t}N(t)\varsigma(t) &= \dot{N}(t)\varsigma(t) + N(t)\dot{\varsigma}(t)\\ &= -\bar{A}^\top(t)N(t)\varsigma(t) - N(t)\bar{A}(t)\varsigma(t) + C^\top C\varsigma(t)\\ &\quad - N(t)QN(t)\varsigma(t) + N(t)\bar{A}(t)\varsigma(t)\\ &= -\Big(\bar{A}(t) + QN(t)\Big)^\top N(t)\varsigma(t) + C^\top y_1(t).\end{aligned}$$

Since $\dot{\psi}(t) = \dot{N}(t)\varsigma(t) + N(t)\dot{\varsigma}(t)$, $\psi(t) \equiv N(t)\varsigma(t)$ holds if they coincide at one point. This is the case at $t = t_0$ with the given initial conditions $N(t_0) = 0$ and $\psi(t_0) = 0$. The equivalence holds regardless of $\varsigma(t_0)$.

The second property (A.2) follows from the uniform complete constructibility of (7). Since (11) is (7) after the change of coordinates (9), the constructibility of the later implies the one of the first. We can identify $N(t)$ and its dynamics in (14) with $P(t)$ in [21, Eq. 1.2] by making $F(t) = -\bar{A}^\top(t)$, $H^\top H = Q$ and $G = C^\top$. If the pair $(\bar{A}(t), C)$ is uniformly completely constructible, the pair $(-\bar{A}^\top(t), C^\top)$ is uniformly completely controllable. Given that $Q > 0$, the pair $(-\bar{A}^\top(t), Q^{1/2})$ is uniform completely observable for arbitrary $\bar{A}(t)$. Under these circumstances, Theorem 2.1 in [21] holds, meaning that $N(t)$ accepts a lower bound of the form (A.2) for some $\bar{\eta} > 0$.

Now we proceed with the proof of Theorem 1. The equivalence (A.1) implies that $N(t)\hat{\xi}(t) - \psi(t) = N(t)\tilde{\xi}(t)$, with $\tilde{\xi}(t) = \hat{\xi}(t) - \varsigma(t)$. This relationship, together with (11) and (12), yield the error dynamics

$$\dot{\tilde{\xi}}(t) = \Big(\bar{A}(t) - K(t)C\Big)\tilde{\xi}(t) - N(t)\sum_{i=1}^{2} r_i \lceil N(t)\tilde{\xi}(t)\rfloor^{p_i}. \tag{A.3}$$

Note that $\bar{A}(t) - K(t)C$, with $K(t)$ as in (13), corresponds to

$$\bar{A}(t) - K(t)C = -\begin{bmatrix}\kappa_1 + u(t) & 0 & 0\\ 0 & u(t) & 0\\ 0 & 0 & 0\end{bmatrix} + \begin{bmatrix}0 & \mu_1(y_1(t)) & u(t) - \mu_1(y_1(t))\xi(t)\\ -\mu_1(y_1(t)) & 0 & 0\\ -u(t) + \mu_1(y_1(t))\xi(t) & 0 & 0\end{bmatrix}, \tag{A.4}$$

where the second matrix is skew-symmetric.

To analyze the observer convergence, we study the Lyapunov stability of (A.3). For that, consider the Lyapunov function candidate $V(\tilde{\xi}) = \tilde{\xi}^\top\varsigma$. Let $\tilde{\xi} = [\tilde{\xi}_1 \ \tilde{\xi}_2]^\top$ and consider (A.4). The derivative of $V(\tilde{\xi})$ along the trajectories of (A.3) is

$$\begin{aligned}\dot{V}(t) &= -2\big(\kappa_1 + u(t)\big)\tilde{\xi}_1(t) - 2u(t)\tilde{\xi}_2(t)\\ &\quad -2\sum_{i=1}^{2} r_i\big(N(t)\tilde{\xi}(t)\big)^\top \lceil N(t)\tilde{\xi}(t)\rfloor^{p_i} \le 0.\end{aligned} \tag{A.5}$$

Since $\dot{V}(t) \le 0$, we conclude from [24, Thm. 4.10] that the origin of (A.3) is uniformly stable. Note that (A.5) holds regardless of Assumption 3 since $\big(N(t)\tilde{\xi}(t)\big)^\top \lceil N(t)\tilde{\xi}(t)\rfloor^{p_i} \ge 0$ for any $N(t)$.

To show the uniform fixed-time convergence of the estimate, we show that $\tilde{\xi} = 0$ is an uniformly fixed-time stable equilibrium point. For this, first denote by $(N(t)\tilde{\xi}(t))_j$ the j-element of the vector $N(t)\tilde{\xi}(t) \in \mathbb{R}^3$. Hence

$$\big(N(t)\tilde{\xi}(t)\big)^\top \lceil N(t)\tilde{\xi}(t)\rfloor^{p_i} = \sum_{j=1}^{3}(N(t)\tilde{\xi}(t))_j \lceil (N(t)\tilde{\xi}(t))_j\rfloor^{p_i}$$

$$= \sum_{j=1}^{3}\big|(N(t)\tilde{\xi}(t))_j\big|^{p_i+1} = \big\|N(t)\tilde{\xi}(t)\big\|_{p_i+1}^{p_i+1}.$$

Given the equivalence between norms in $\mathbb{R}^n$, there exist positive constants c_1 and c_2 such that $\|\nu\|_{p_i+1} \ge c_i\|\nu\|$ for any $\nu \in \mathbb{R}^n$. Therefore, from the norm equivalence and (A.5) we have

$$\dot{V}(t) \le -2u(t)\big(\tilde{\xi}_1(t) + \tilde{\xi}_2(t)\big) - 2\sum_{i=1}^{2} r_i c_i \big\|N(t)\tilde{\xi}(t)\big\|^{p_i+1}.$$

We can further bound $\dot{V}(t)$ by introducing the lower bound of $N(t)$ in (A.2). Therefore, for $t \ge t_0 + T_1$, we have

$$\dot{V}(t) \le -2u(t)\big(\tilde{\xi}_1(t) + \tilde{\xi}_2(t)\big) - 2\sum_{i=1}^{2} r_i c_i \bar{\eta}^{p_i+1}\|\tilde{\xi}(t)\|^{p_i+1}.$$

Neglect the semi-definite term, and note that $V^{1/2}(t) = \|\tilde{\xi}(t)\|$. Thus we obtain

$$\dot{V}(t) \le -2\sum_{i=1}^{2} r_i c_i \bar{\eta}^{p_i+1} V^{\frac{p_i+1}{2}}(t) < 0. \tag{A.6}$$

Note that $\frac{1}{2}(p_1 + 1) < 1$ and that $\frac{1}{2}(p_2 + 1) > 1$ since $p_1 \in [0, 1)$ and $p_2 > 1$. To solve the differential inequality (A.6) we use the Comparison Lemma [24, Lem. 3.4] together with the following differential equation and its solution:

$$\begin{aligned}&\dot{v}(t) = -a\, v^\alpha(t),\ v(t_0) \ge 0,\ \alpha \ge 0,\ \alpha \ne 1,\\ &v^{1-\alpha}(t) = \max\Big\{v^{1-\alpha}(t_0) - a(1-\alpha)\big(t - t_0\big),\ 0\Big\}.\end{aligned} \tag{A.7}$$

Since (A.6) holds for each term in the sum, we simultaneously have

$$V(t) \le \Big(V^{\frac{1-p_i}{2}}(t_0) - \big(1 - p_i\big)r_i c_i \bar{\eta}^{p_i+1}\big(t - t_0\big)\Big)^{\frac{2}{1-p_i}}. \tag{A.8}$$

Without loss of generality, assume that $V(t_0) > 1$. We investigate the required time to ensure $1 \ge V(t)$. For that, consider (A.8) with $i = 2$. It follows that

$$V(t) \le \frac{1}{\left(\frac{1}{V^{\frac{p_2-1}{2}}(t_0)} + \big(p_2 - 1\big)r_2 c_2 \bar{\eta}^{p_2+1}\big(t - t_0\big)\right)^{\frac{2}{p_2-1}}} \le 1$$

holds for

$$t - t_0 \ge \frac{1}{(p_2 - 1)r_2 c_2 \bar{\eta}^{p_2+1}}\left(1 - \frac{1}{V^{\frac{p_2-1}{2}}(t_0)}\right). \tag{A.9}$$

For arbitrarily large $V(t_0)$, $1 \ge V(t)$ can be guaranteed for

$$t - t_0 \ge 1/(r_2 c_2 \bar{\eta}^{p_2+1}(p_2 - 1)).$$

This represents an upper bound for the amount of time needed. Furthermore, note that it is finite and independent of the initial condition. Now, we investigate the time needed to guarantee $V(t) = 0$ starting from $V(t_0) = 1$. For that, consider (A.8) with $i = 1$. Hence

$$V^{\frac{1-p_1}{2}}(t) \le 1 - \big(1 - p_1\big)r_1 c_1 \bar{\eta}^{p_1+1}\big(t - t_0\big) \le 0 \tag{A.10}$$

$$\frac{1}{r_1 c_1 \bar{\eta}^{p_1+1}(1 - p_1)} \le t - t_0. \tag{A.11}$$

Using (A.9) and (A.11), we can estimate the maximum time $t^\star$ for which it holds $V(t) = 0$ for all $t \ge t^\star$. This time corresponds to

$$t^\star - t_0 = \frac{1}{r_1 c_1 \bar{\eta}^{p_1+1}(1 - p_1)} + \frac{1}{r_2 c_2 \bar{\eta}^{p_2+1}(p_2 - 1)}.$$

Since the difference $t^\star - t_0$ does not depend on the initial time, or the initial value $V(t_0)$, we conclude that the origin of the system (A.3) is uniformly fixed-time stable.

Finally, the estimate of the original variables follows from the inverse relation to (9). □

A.2. Proof of Proposition 1

Consider the system (7). By applying the output feedback $\bar{K}(t)\bar{y}_1(t)$, where

$$\bar{K} = \begin{bmatrix} u(t) - \mu_1(y_1(t)) & -\frac{1}{a}\big(u(t) - \mu_1(y_1(t))\big) & 0 \end{bmatrix}^\top,$$

and the change of coordinates $\bar{\chi}(t) = T\,\chi(t)$, where

$$T = \begin{bmatrix} 1 & 0 & 0 \\ 1 & a & -1 \\ 0 & 0 & 1 \end{bmatrix},\ T^{-1} = \begin{bmatrix} 1 & 0 & 0 \\ -1/a & 1/a & 1/a \\ 0 & 0 & 1 \end{bmatrix},$$

we obtain the system description

$$\begin{aligned} \dot{\bar{\chi}}(t) &= \Big(T\big(A(t) + \bar{K}(t)C\big)T^{-1}\Big)\bar{\chi}(t) \\ &= \begin{bmatrix} 0 & -\mu_1(y_1(t)) & u(t) - \mu_1(y_1(t)) \\ 0 & -u(t) & 0 \\ 0 & 0 & 0 \end{bmatrix}\bar{\chi}(t), \qquad \text{(A.12)} \\ \bar{y}_1(t) &= CT^{-1}\bar{\chi}(t) = \begin{bmatrix} 1 & 0 & 0 \end{bmatrix}\bar{\chi}(t). \end{aligned}$$

Note that a bounded output injection does not change the observability properties of a system [27]. Therefore, we can investigate the uniform completely observability of (7) by means of (A.12).

The advantage of expressing the system in the form (A.12) is that we can compute the system response directly. This results in

$$\begin{aligned} \bar{y}_1(t) = \bar{\chi}_1(t_0) + \bar{\chi}_3(t_0)\int_{t_0}^{t}\Big(u(s) - \mu_1(y_1(s))\Big)\mathrm{d}s \\ - \bar{\chi}_2(t_0)\int_{t_0}^{t}\mu_1(y_1(s))\exp\left(-\int_{t_0}^{s}u(\sigma)\mathrm{d}\sigma\right)\mathrm{d}s. \qquad \text{(A.13)} \end{aligned}$$

Note that

$$\int_{t}^{t+T_1}\bar{y}_1^2(s)\mathrm{d}s = \bar{\chi}^\top(t)\mathcal{M}(t+T_1, t)\bar{\chi}(t),$$

where $\mathcal{M}(t+T_1, t)$ is the observability Gramian of the system. Thus, from (A.13) we obtain

$$\mathcal{M}(t+T_1, t) = \int_{t}^{t+T_1}\begin{bmatrix} 1 & \mathcal{K}(s,t) \\ \mathcal{K}^\top(s,t) & \mathcal{K}^\top(s,t)\mathcal{K}(s,t) \end{bmatrix}\mathrm{d}s, \qquad \text{(A.14)}$$

with $\mathcal{K}(s,t)$ defined in (16). Note that we can identify $B(t,t_0)$ in (16) with $V(t)$ in [28, Thm. 2] and $\mathcal{M}(t+T_1,t)$ in (A.14) with $N(t+T_1,t)$ in [28, Thm. 2]. Thus, following the main result of [28, Thm. 2], we can conclude that the system (7) is uniformly completely observable iff (15) holds. □

A.3. Proof of Theorem 2

Let $\tilde{x}_2(t) = \hat{x}_2(t) - x_2(t)$. In account of (17) and (18) we have that

$$\dot{\tilde{x}}_2(t) = -u(t)\tilde{x}_2(t). \qquad \text{(A.15)}$$

To study the stability of the origin of (A.15), we borrow the following Lyapunov function from [29, Eq. 4]

$$V_2(\tilde{x}_2, t) = \left(\frac{T_2^2 u_{\max}^2 \gamma_3^2}{\gamma_4} + \frac{T_2}{2} + \int_{t-T_2}^{t}(\tau - t + T_2)u^2(\tau)\mathrm{d}\tau\right)\tilde{x}_2^2.$$

Following [29], we have

$$\beta_1\tilde{x}_2^2 \geq V_2(\tilde{x}_2, t) \geq \beta_2\tilde{x}_2^2,$$

with $\beta_1 > 0$ and $\beta_2 > 0$ as in (21). Furthermore, it follows that

$$\dot{V}_2(t) \leq -\frac{\gamma_4}{2}\tilde{x}_2^2(t). \qquad \text{(A.16)}$$

By invoking [24, Thm. 4.10], we conclude that the origin of (A.15) is uniformly exponentially stable. Thus, the observer converges exponentially fast.

To estimate the rate of convergence, we first change (A.16) into a differential inequality by using (21):

$$\dot{V}_2(t) \leq -\frac{\gamma_4}{2\beta_2}V_2(t),$$

whose solution is

$$V_2(t) \leq V_2(t_0)\exp\left(-\frac{\gamma_4}{2\beta}(t - t_0)\right).$$

Using the bounds (21) once more, the inequality (20) follows, concluding the proof. □

A.4. Proof of Theorem 3

First, we compute the dynamics of the estimation errors $\tilde{z}(t) = \hat{z}(t) - z(t)$ and $\tilde{\zeta}(t) = \hat{\zeta}(t) - \zeta(t)$. This results in

$$\begin{aligned} \dot{\tilde{z}}(t) &= -k_1 u(t)\phi_1\big(\tilde{z}(t)\big) + u(t)\tilde{\zeta}(t), \\ \dot{\tilde{\zeta}}(t) &= -k_2 u(t)\phi_2\big(\tilde{z}(t)\big) - \dot{\sigma}_2(t). \end{aligned} \qquad \text{(A.17)}$$

Note that $\dot{\zeta}(t) = \dot{\sigma}_2(t)$ since $\zeta(t) = c/a\,\sigma_1 + \sigma_2(t)$ and that σ_1 is assumed constant according to Assumtion 2. 1.

To continue, we investigate the stability of the origin of (A.17) to show the convergence of the observer. Since the dilution rate $u(t)$ is non-negative, it does not change its sign. Therefore, we can follow [22, Sec. 3.1] to analyze the system stability. According to this, define $\varkappa(t) = [\phi_1\big(\tilde{z}(t)\big)\ \ \tilde{\zeta}(t)]^\top$ and consider the Lyapunov function

$$V_3(\varkappa) = \varkappa^\top\begin{bmatrix} \rho_1 & -1 \\ -1 & \rho_2 \end{bmatrix}\varkappa, \qquad \text{(A.18)}$$

which is positive definite for ρ_1 and ρ_2 as in (24). Furthermore, $V_3(\varkappa)$ is absolutely continuous and continuously differentiable everywhere except on the set $\mathcal{D} = \{(\tilde{z}, \tilde{\zeta}) \in \mathbb{R}^2 \mid \tilde{z} = 0\}$ [22]. Consider the gradient components of $V_3(\varkappa)$:

$$\frac{\partial V_3}{\partial \tilde{z}} = 2\rho_1\phi_1\big(\tilde{z}\big)\phi_1'\big(\tilde{z}\big) - 2\tilde{\zeta}\phi_1'\big(\tilde{z}\big), \quad \frac{\partial V}{\partial \tilde{\zeta}} = 2\rho_2\tilde{\zeta} - 2\phi_1\big(\tilde{z}\big),$$

where

$$\phi_1'\big(\tilde{z}\big) = \frac{1}{2}m_1|\tilde{z}|^{-\frac{1}{2}} + p_3 m_2|\tilde{z}|^{p_3 - 1} > 0. \qquad \text{(A.19)}$$

In the set $\mathbb{R}^2 \setminus \mathcal{D}$, the derivative of $V_3(\varkappa)$ along the trajectories of (A.17) corresponds to

$$\begin{aligned} \dot{V}_3(t) &= \frac{\partial V_3}{\partial \tilde{z}}(t)\dot{\tilde{z}}(t) + \frac{\partial V_3}{\partial \tilde{\zeta}}(t)\dot{\tilde{\zeta}}(t) \\ &= -2u(t)\phi_1'(\tilde{z}(t))\Big(\tilde{\zeta}^2(t) - (k_1 + \rho_1 - k_2\rho_2)\phi_1(\tilde{z}(t))\tilde{\zeta}(t) \\ &\quad + (k_1\rho_1 - k_2)\phi_1^2(\tilde{z}(t))\Big) + 2\dot{\sigma}_2(t)\Big(\phi_1(\tilde{z}(t)) - \rho_2\tilde{\zeta}(t)\Big), \end{aligned}$$

where the relation $\phi_2(\tilde{z}) = \phi_1'(\tilde{z})\phi_1(\tilde{z})$ was used. Let $\alpha(t, \varkappa(t))$ be an auxiliary function satisfying

$$\dot{\sigma}_2(t) = \frac{2L}{m_1^2}(t)\phi_2\big(\tilde{z}(t)\big)\alpha(t, \varkappa(t)),\ \ 1 \geq \big|\alpha(t, \varkappa(t))\big|.$$

Such function exists in account of Assupmtion 2. 2 and the fact that for $\tilde{z} \neq 0$ we have $|\phi_2(\tilde{z})| \geq m_1^2/2$. Using $\alpha(t, \varkappa(t))$ and (23), we can rewrite $\dot{V}_3(t)$ as

$$\dot{V}_3(t) = -2u(t)\phi_1'\big(\tilde{z}(t)\big)\,\varkappa^\top(t)\,Q\big(t, \varkappa(t)\big)\,\varkappa(t), \qquad \text{(A.20)}$$

with

$$Q\left(t,\varkappa(t)\right)=\begin{bmatrix} l_1+\frac{2L\alpha(t,\varkappa(t))}{m_1^2} & \frac{1}{2}\left(l_2-\rho_1-\rho_2\frac{2L\alpha(t,\varkappa(t))}{m_1^2}\right)\\ \star & 1\end{bmatrix}. \tag{A.21}$$

Proving that $\dot{V}(t)$ is negative semi-definite reduces to show that $Q\left(t,\varkappa(t)\right)\geq 0$ for all $\xi\in\mathbb{R}^2\setminus\mathcal{D}$ and $t\geq t_0$. This can be investigated using the Schur complement, from which we have

$$\left(l_1+\frac{2L\alpha(t,\varkappa(t))}{m_1^2}\right)>\frac{1}{4}\left(l_2-\rho_1-\rho_2\frac{2L\alpha(t,\varkappa(t))}{m_1^2}\right)^2,$$

or

$$l_1>\frac{2L}{m_1^2}+\frac{1}{4}\left(l_2-\rho_1+\rho_2\frac{2L\alpha(t,\varkappa(t))}{m_1^2}\right)^2. \tag{A.22}$$

Since $\alpha(t,\varkappa(t))$ can be written as the convex combination

$$\alpha(t,\varkappa(t))=-\lambda(t)+(1-\lambda(t)),\ \lambda(t)\in[0,1],$$

it is enough to satisfy (A.22) in the extremes. This corresponds to (24). Therefore, $V_3(\varkappa(t))$ is non-increasing, and the origin is uniformly stable. Following [22,30] and for $\frac{1}{2}\leq p_3\leq 1$, the expression (A.20) can be transformed into the differential inequality

$$V_3(t)\leq-\alpha_1u(t)V_3^{\frac{1}{2}}(t)-\alpha_2u(t)V_3^{\frac{3p_3-1}{2p_3}}(t), \tag{A.23}$$

with

$$\lambda_Q=\min_{t,\xi}\lambda_{\min}\left(Q\left(t,\varkappa(t)\right)\right),$$

$$\alpha_1=m_1^2\frac{\lambda_{\min}^{\frac{1}{2}}(P)\lambda_Q}{2\lambda_{\max}(P)},\quad \alpha_2=m_2^{\frac{1}{p_3}}\frac{p_3\lambda_{\min}^{\frac{1-p_3}{2p_3}}(P)\lambda_Q}{\lambda_{\max}(P)}.$$

From here and the Comparison Lemma [24, Lem. 3.4], the evolution of $V_3(\varkappa(t))$ can be bounded as (see [22])

$$V_3^{\frac{1}{2}}(t)\leq\max\left\{V^{\frac{1}{2}}(t_0)-\frac{1}{2}\alpha_1\int_{t_0}^{t}u(\sigma)\mathrm{d}\sigma,0\right\}.$$

Hence, if the integral of $u(t)$ diverges, there is a time $t^\star<\infty$ for which $V_3(t)=0$ for $t\geq t^\star$, meaning that the origin of (A.17) is finite-time stable. This happens if, for example, (19) holds. The persistency of excitation condition (19) implies the existence of constants $\varepsilon_1>0$ and $\varepsilon_2\in\mathbb{R}$, both independent of t, such that [31, Thm. 1]

$$\int_{t_0}^{t}u(\sigma)\mathrm{d}\sigma\geq\varepsilon_1\left(t-t_0\right)+\varepsilon_2.$$

Using this expression, $t^\star$ can be estimated as

$$t^\star=t_0+\frac{2}{\varepsilon_1\alpha_1}V_3^{\frac{1}{2}}(t_0)-\frac{\varepsilon_2}{\varepsilon_1}.$$

The persistency of excitation also makes the difference $t^\star-t_0$ independent of the initial time, meaning that the stability is uniform. Thus, we conclude that the origin of (A.17) is uniformly finite-time stable under these circumstances. This is translated into the uniform finite-time convergence of the observer.

Finally, the estimates of the original variables follows from the inverse relation to (4). □

References

[1] IWA Task Group for Mathematical Modelling of Anaerobic Digestion Processes, Anaerobic Digestion Model No. 1 (ADM1), IWA Publishing, London, 2005.

[2] J.L. Montiel-Escobar, V. Alcaraz-Gonzalez, H. Mendez-Acosta, V. Gonzalez-Alvarez, ADM1-based robust interval observer for anaerobic digestion processes, Clean Soil Air Water 40 (2012) 933–940.

[3] O. Bernard, Z. Hadj-Sadok, D. Dochain, A. Genovesi, J.-P. Steyer, Dynamical model development and parameter identification for an anaerobic wastewater treatment process, Biotechnol. Bioeng. 75 (4) (2001) 424–438.

[4] D. Theilliol, J.-C. Ponsart, J. Harmand, C. Join, P. Gras, On-line estimation of unmeasured inputs for anaerobic wastewater treatment processes, Control Eng. Pract. 11 (2003) 1007–1019.

[5] E. Jauregui-Medina, V. Alcaraz-Gonzalez, H. Mendez-Acosta, V. Gonzalez-Alvarez, Observer-based input estimation in continuous anaerobic wastewater treatment processes, Water Sci. Technol. 60 (2009) 805–812.

[6] A. Rodríguez, G. Quiroz, R. Femat, H. Méndez-Acosta, J. de León, An adaptive observer for operation monitoring of anaerobic digestion wastewater treatment, Chem. Eng. J. 269 (2015) 186–193.

[7] M. Sbarciog, J.A. Moreno, A. Vande Wouwer, Application of super-twisting observers to the estimation of state and unknown inputs in an anaerobic digestion system, Water Sci. Technol. 69 (2014) 414–421.

[8] S. Attar, F. Haugen, Dynamic model adaptation to an anaerobic digestion reactor of a water resource recovery facility, Model. Identif. Control 40 (3) (2019) 143–160.

[9] J.A. Moreno, D. Dochain, Global observability and detectability analysis of uncertain reaction systems and observer design, Internat. J. Control 81 (7) (2008) 1062–1070.

[10] V. Alcaraz-Gonzalez, J. Harmand, A. Rapaport, J. Steyer, V. Gonzalez-Alvarez, C. Pelayo-Ortiz, Software sensors for highly uncertain WWTPs: a new approach based on interval observers, Water Res. 36 (2002) 2515–2524.

[11] M. Moisan, O. Bernard, J.-L. Gouzé, A high/low gain bundle of observers: application to the input estimation of a bioreactor model, IFAC Proc. Vol. 41 (2) (2008) 15547–15552, 17th IFAC World Congress.

[12] L. Dewasme, M. Sbarciog, E. Rocha-Cózatl, F. Haugen, A. Vande Wouwer, State and unknown input estimation of an anaerobic digestion reactor with experimental validation, Control Eng. Pract. 85 (2019) 280–289.

[13] S. Nuñez, H. De Battista, F. Garelli, A. Vignoni, J. Picó, Second-order sliding mode observer for multiple kinetic rates estimation in bioprocesses, Control Eng. Pract. 21 (9) (2013) 1259–1265.

[14] A. Vargas, J.A. Moreno, A. Vande Wouwer, A weighted variable gain super-twisting observer for the estimation of kinetic rates in biological systems, J. Process Control 24 (6) (2014) 957–965, Energy Efficient Buildings Special Issue.

[15] J.A. Moreno, I. Mendoza, Application of super-twisting-like observers for bioprocesses, in: 2014 13th International Workshop on Variable Structure Systems (VSS), 2014, pp. 1–6.

[16] J.A. Moreno, J. Alvarez, On the estimation problem of a class of continuous bioreactors with unknown input, J. Process Control 30 (2015) 34–49.

[17] J.A. Moreno, Lyapunov approach for analysis and design of second order sliding mode algorithms, in: L. Fridman, J. Moreno, R. Iriarte (Eds.), Sliding Modes After the First Decade of the 21st Century, Vol. 412, Springer, 2011, pp. 113–150.

[18] W.M. Haddad, S.G. Nersesov, Liang Du, Finite-time stability for time-varying nonlinear dynamical systems, in: 2008 American Control Conference, 2008, pp. 4135–4139.

[19] A. Polyakov, L. Fridman, Stability notions and Lyapunov functions for sliding mode control systems, J. Franklin Inst. B 351 (4) (2014) 1831–1865.

[20] J. Jimenez, E. Latrille, J. Harmand, A. Robles, J. Ferrer, D. Gaida, C. Wolf, F. Mairet, O. Bernard, V. Alcaraz-Gonzalez, H. Mendez-Acosta, D. Zitomer, D. Totzke, H. Spanjers, F. Jacobi, A. Guwy, R. Dinsdale, G. Premier, S. Mazhegrane, G. Ruiz-Filippi, A. Seco, T. Ribeiro, A. Pauss, J.-P. Steyer, Instrumentation and control of anaerobic digestion processes: a review and some research challenges, Rev. Environ. Sci. Bio/Technol. 14 (2015) 615–648.

[21] R.S. Bucy, The Riccati equation and its bounds, J. Comput. System Sci. 6 (4) (1972) 343–353.

[22] E. Guzmán, J.A. Moreno, Super-twisting observer for second-order systems with time-varying coefficient, IET Control Theory Appl. 9 (4) (2015) 553–562.

[23] A.F. Filippov, Differential Equations with Discontinuous Right-Hand Side, Kluwer Academic Publishers, P.O. Box 17, 3300 AA Dordrecht, The Netherlands, 1988.

[24] H. Khalil, Nonlinear Systems, third ed., Prentice–Hall, New Jersey, 2002.

[25] F. Lopez-Ramirez, D. Efimov, A. Polyakov, W. Perruquetti, Finite-time and fixed-time input-to-state stability: Explicit and implicit approaches, Systems Control Lett. 144 (2020) 104775.

[26] R.N. Páscoa, J.A. Lopes, J.L. Lima, In situ near infrared monitoring of activated dairy sludge wastewater treatment processes, J. Near Infrared Spectrosc. 16 (4) (2008) 409–419.

[27] L. Zhang, Q. Zhang, Observability conservation by output feedback and observability Gramian bounds, Automatica 60 (2015) 38–42.
[28] B.D.O. Anderson, Exponential stability of linear equations arising in adaptive identification, IEEE Trans. Automat. Control 22 (1) (1977) 83–88.
[29] J.G. Rueda-Escobedo, J.A. Moreno, Strong Lyapunov functions for two classical problems in adaptive control, Automatica (2020) 109250.
[30] J.A. Moreno, Lyapunov approach for analysis and design of second order sliding mode algorithms, in: L. Fridman, J. Moreno, R. Iriarte (Eds.), Sliding Modes After the First Decade of the 21st Century, Springer-Verlag, Berlin Heidelberg, 2011, pp. 113–150.
[31] A.P. Morgan, K.S. Narendra, On the uniform asymptotic stability of certain linear nonautonomous differential equations, SIAM J. Control Optim. 15 (1) (1977) 5–24.